Proceedings of Combustion Institute - Canadian Section
Spring Technical Meeting
University of Waterloo, Waterloo
May 10-12, 2016

Numerical investigation of Doubly Conditional Source-Term Estimation applied to turbulent partially premixed combustion

M. Mortada and C.B. Devaud*

Department of Mechanical and Mechatronics Engineering, University of Waterloo
200 University Avenue West, Waterloo, Ontario, N2L3G1, Canada

Abstract

Flame stabilization remains a crucial issue for good operation of engines, industrial furnaces and flares. The present study is focused on a series of lifted turbulent jet flames stabilized in cold air at three different Re 7000, 12000, and 19500. In these conditions, the flame stabilization involves the propagation of a partially premixed flame. The present work revisits the implementation of Doubly Conditional Source-term Estimation (DCSE) applied to lifted turbulent flames burning methane. The objectives of the present study are to implement a more advanced scalar dissipation rate model for better description of mixing, and to examine computational time reduction methods. In contrast to the commonly used algebraic expression, the new scalar dissipation rate model is developed specifically for partially premixed combustion. A different algorithm for solving sparse least squares is considered, instead of the time-consuming LU-decomposition originally implemented. The simulations are performed using a Reynolds Averaged Navier Stokes approach with the $k-\varepsilon$ turbulence model. Detailed chemistry is included. Methane concentration profiles are well-predicted at the lowest Re. The scalar dissipation rate model is found to have a clear impact on the lift-off height predictions, in particular for the two highest Reynolds numbers. The results obtained using LSQR algorithm in the simulations show a significant time saving retaining good accuracy of solution.

1. INTRODUCTION

Lifted flame can be observed when the fuel injection increases over a certain value that prevents the flame from stabilizing at the burner rim. The flame lift-off height is measured between the flame base and the rim of the burner. Lifted flames can be found in many industrial applications like flares, commercial boilers, and diesel engines [1].

Recent experimental investigations show that partially premixed flame propagation is a plausible explanation for flame stabilization for lifted flames in cold surroundings [2–5]. Numerically, the combination of premixed/non-premixed approaches have been investigated in the flamelet context to include the effect of partially premixed flame propagation. For example, Bradley et al. [6] report good agreement with experimental results, but their formulation relies on premixed flame propagation. Further improvement is considered by adding some modifications allowing for premixed flame extinction [7]. In a different version of the flamelet model, mixture fraction that indicates the equivalence ratio, and variable G that tracks the location of the flame front are used together with good results for the lift-off height prediction [8].

The Conditional Source-term Estimation (CSE) approach has been recently applied to a series of lifted flames in cold air using Reynolds Averaged Navier Stokes (RANS) simulations with good predictions for the lift-off height [9]. In CSE, an integral equation must be inverted to obtain the conditional moments such conditional species mass fractions. The advantages of CSE are that the model is not restricted to any specific combustion regime and no additional closure is needed to determine the conditional scalars. In order to include the partially-premixed flame propagation, doubly conditioning is considered leading to Doubly Conditional Source-term Estimation (DCSE). In the previous DCSE calculations [9], a simple linear relaxation scalar dissipation rate model is used in the progress variable variance equation, which is shown to be inaccurate, even in premixed conditions, and does not take into consideration the partially premixed configuration [10]. In the present work, a more advanced scalar dissipation rate formulation [11] is implemented. Further, with the perspective of running Large Eddy Simulation (LES) with DCSE, the computational time needs to be reduced as much as possible. Thus, a different numerical technique is investigated to solve the inverted integral equation. In particular, the Least Squares QR-factorization (LSQR) algorithm instead of LU-decomposition, is examined. The LSQR algorithm has been recently assessed [12] and shown to gain significant computational time-saving for relatively small matrices.

The objectives of the present paper are to investigate the effect of an advanced scalar dissipation rate model on the lift-off height

*Corresponding author: cdevaud@uwaterloo.ca Tel: +1 (519) 888-4567 ext. 36094

predictions of a series of lifted turbulent jet flames, and to obtain an assessment of the LSQR algorithm in solving the minimization problem included in the integral equation inversion process over the use of the default LU-decomposition algorithm. The assessment includes the time consumption and the accuracy retained for each numerical method.

2. DCSE formulation

In the present formulation, DCSE uses mixture fraction and a reaction progress variable as conditioning variables for the conditional averaged scalars. The unconditional averages can be determined by double-integrating the conditional averaged scalar multiplied by the presumed Favre-averaged Probability Density Function (PDF) over the mixture fraction and progress variable sample space as follows

$$\underbrace{\tilde{f}(\vec{x},t)}_{\text{Favre average}} = \int\int \underbrace{\overline{f|\eta,c^*}(\eta,c^*;\vec{x},t)}_{\text{conditional average}} \underbrace{\tilde{P}(\eta,c^*;\vec{x},t)}_{\text{Joint PDF}} d\eta dc^*, \tag{1}$$

where f may be any scalar, t is time, $\vec{x}$ the spatial location vector, η the mixture fraction sample space, and c^* the progress variable sample space. It has been observed that the conditional averages vary much less in physical space compared to the unconditional averages [13]. Thus, the conditional averages are considered space invariant for each ensemble (ensembles will be defined in Section 3), and Eq. 1 becomes

$$\tilde{f}(\vec{x}_j,t) = \int\int \overline{f|\eta,c^*}(\eta,c^*;t)\tilde{P}(\eta,c^*;\vec{x}_j,t)d\eta dc^* \quad j \in J, \tag{2}$$

where $\vec{x}_j$ is the spatial coordinate of the j-th point in the ensemble J. By discretizing Eq. 2, the following form is obtained

$$\int_{\eta_1}^{\eta_2}\int_{{c^*}_1}^{{c^*}_2} \overline{f|\eta,c^*}(\eta,c^*;t)\tilde{P}(\eta_m,c^*_m;\vec{x}_j,t)d\eta dc^*, \tag{3}$$

where m indicates the index of the sample point within the sample interval (bin), and η_1, η_2, ${c^*}_1$, ${c^*}_2$ are the lower and upper bounds of the bin for mixture fraction and progress variable, respectively. In the case of DCSE, the combined mixture fraction/progress variable space is composed of (n_η x n_c) points where n_η is the number of points in mixture fraction space and n_c the number of points in the progress variable space. Eq. 3 can be cast in matrix form as $A\,\vec{\alpha} = \vec{b}$, where A is a (N x M) matrix where N is the number of grid points in the ensemble and M the number of bins in the combined mixture fraction/progress variable space, $\vec{\alpha}$ is the conditional averaged scalar vector of size M for a given ensemble, and $\vec{b}$ is the unconditional averaged scalar vector of size N.

Matrix A represents the integrated joint PDF which is a function of mixture fraction and progress variable as well as space and time. The generated A matrix is larger than its counterpart in non-premixed [14–16] and premixed flames [17, 18]. Thus, the inversion process is expected to be more computationally expensive,

$$\vec{\alpha} = A^{-1}\vec{b}. \tag{4}$$

The solution for $\vec{\alpha}$ is ill-posed. Therefore, it is sensitive to small perturbations [19]. To get a unique smooth solution, regularization is required. The regularization approach involves solving the minimization problem,

$$\vec{\alpha} = \arg\min\left\{ \left\| \mathbf{A}\vec{\alpha} - \vec{b} \right\|_2^2 + \lambda^2 \left\| \vec{\alpha} - \vec{\alpha}_0 \right\|_2^2 \right\}, \tag{5}$$

where $\|..\|_2$ represents L2-norm, λ is the regularization parameter, $\vec{\alpha}_0$ the *a priori* knowledge which is often selected as the solution from the previous time-step. The regularization parameter is determined by $\lambda=\frac{Tr(A^TA)}{Tr(I)}$ [15], where I is the identity matrix of the same dimensions as $A^T A$, and Tr is the trace of a matrix. The joint PDF is obtained using Bayes theorem, $\tilde{P}(\eta,c^*)=\tilde{P}(\eta)\ \tilde{P}(c^*|\eta)$ where $\tilde{P}(\eta)$ is calculated using a β-PDF [20], and $\tilde{P}(c^*)$ calculated modified laminar flamelet PDF [21] at a given equivalence ratio or mixture fraction. For some fuel lean and rich conditions outside the flammability limits, the β-PDF is used for $\tilde{P}(c^*|\eta)$, instead of the modified laminar flamelet PDF.

In the present study, two solution methods are adopted to perform the inversion process with zeroth-order Tikhonov regularization [22]. The first technique is the LU-decomposition which is originally used with CSE to solve the system of over-determined least squares in Eq. 5. The second technique is LSQR which is an iterative numerical method [23]. This method employs Lanczos method that leads to a factorization of the tridiagonal reduced matrix of $A^T A$. It is used to solve over- and under-determined system of equations and minimization problems. The method is based on the bidiagonalization procedure used for sparse and large A matrix of Golub and Kahan [24]. It is similar to the method of conjugate gradients, except for having more favorable numerical properties [23]. The time consumption is primarily dependent on the matrix-vector multiplications $A\ \vec{\alpha}$ of and $A^T\ \vec{b}$ [12].

3. Computational Details

The computational domain closely follows the experimental setup [25–27]. The fuel jet diameter is 5.4 mm surrounded by ambient air at coflow conditions assumed to be still air [9]. The jet velocities are equal to 21, 37, and 60 m/s corresponding to Reynolds number values of 7000, 12000, and 19500, respectively. The turbulence intensity at the fuel inlet is taken to be equal to 10% based on the maximum value of centerline velocity fluctuations for jet-velocity equal to 21 m/s and the ratio between the air to methane velocity is taken to be 0.005 [27].

An open source CFD package OpenFOAM [28] is used to solve the governing equations which include conservation of mass, energy, momentum, species mass fraction, mixture fraction and its variance transport equations, and progress variable and its variance transport equations. As the DCSE is implemented in RANS with the k-ε model [29], the transport equations of turbulent kinetic energy and its dissipation are included in the solution. In the present work, detailed chemistry coupled with Trajectory-Generated Low Dimensional Manifold (TGLDM) tabulation technique is adopted [30]. Chemistry is tabulated as a function of two variables; the mass fraction of carbon dioxide and water for given values of mixture fraction and progress variable. Using the conditional moments of the specified mass fractions, the conditional moment of chemical reactions can be retrieved. Then, the unconditional values can be obtained by the integration with the joint PDF over the entire range of the conditioning variables (Eq. 1). The progress variable is selected to be the carbon dioxide mass fraction normalized by its equilibrium value at a given η.

To define the DCSE ensembles, the entire computational domain is divided into planes normal to the centerline. There is a small overlap between adjacent ensembles to prevent any sharp changes in conditional values. For the points that are located in the overlapping area, the final unconditional mean reaction rate is equal to the arithmetic average of the two unconditional values obtained from the two adjacent ensembles. The number of points defined in the ensemble must be at least equal to N to avoid a rank-deficient condition in the inversion problem. The present computational domain is divided into three ensembles as Dovizio et al. [9] show that the difference in predictions with 8 DCSE ensembles is less than 3%.

As shown in Eq. 6, a scalar dissipation rate model is required to close the progress variable fluctuations term, $\overline{\rho D\frac{\partial c''}{\partial x_i}\frac{\partial c''}{\partial x_i}}$, in the transport equation of the progress variable variance.

$$\frac{\partial(\overline{\rho}\tilde{c''^2})}{\partial t}+\frac{\partial}{\partial x_i}(\overline{\rho}\tilde{u}_i\tilde{c''^2})=\frac{\partial}{\partial x_i}(\overline{\rho D\frac{\partial c''^2}{\partial x_i}})-\frac{\partial}{\partial x_i}(\overline{\rho u_i'' c''^2})-2\overline{\rho u_i'' c''}\frac{\partial\tilde{c}}{\partial x_i}-2\overline{\rho D\frac{\partial c''}{\partial x_i}\frac{\partial c''}{\partial x_i}}+2\overline{c''\dot{\omega}_c}, \tag{6}$$

where $\overline{\rho}$ is the mean density, c'' the progress variable fluctuations, u'' the velocity fluctuations, D the progress variable diffusivity and $\dot{\omega}_c$ represents the chemical source term for c determined by DCSE through the TGLDM table. The simple algebraic model given by Eq. 7, presents some weaknesses in describing the reactive scale fluctuations decay adequately.

$$\tilde{x_c}=\overline{\rho D\frac{\partial c''}{\partial x_i}\frac{\partial c''}{\partial x_i}}=\overline{\rho}c_x\frac{\varepsilon}{k}\tilde{c''^2}, \tag{7}$$

where ε is the dissipation of turbulent kinetic energy and k the turbulent kinetic energy. Instead, the model proposed by Kolla et al. [31] is modified to include the effect of equivalence ratio on each term and has been modified and leads to [11]

$$\tilde{x_c}(Z)=2\bar{\rho}\frac{1}{\beta}([2K_{c^*}(Z)-\tau(Z)C_4(Z)]\frac{S_L(Z)}{\delta_L(Z)}+C_3(Z)\frac{\tilde{\varepsilon}}{\tilde{k}})\tilde{c''^2}, \tag{8}$$

where τ is the heat release factor, S_L is the laminar flame speed, , δ_L is the unstrained laminar thermal thickness, $\tilde{k}$ is the mean turbulent kinetic energy, $\tilde{\varepsilon}$ is the mean turbulent dissipation rate, β is the model constant, C_3 and C_4 are functions in Karlovitz number, and K_{c^*} is to be evaluated by the aid of laminar flame results.In Eq. 8, three main contributions can be considered. On the left hand side, the first term represents the correlation between dissipation and dilatation rates. The second term corresponds to the strain due to heat release. The last term indicates the turbulent strain rate and is proportional to the turbulent time scale [31].

4. RESULTS

As an assessment of the advanced scalar dissipation rate model for partially-premixed combustion, cases for the three given Reynolds numbers are run using the same configuration used by Dovizio et al. [9], only changing the scalar dissipation rate model. As shown in Fig.1, predictions obtained for mean methane concentration $\bar{C}_{CH_4}$ remain in good agreement with the experimental data for the case of low Reynolds number (Re = 7000). The experimental methane concentration profiles are only available at Re = 7000. There are different approaches available to estimate the lift-off height from the numerical results. Following the previous DCSE study [9], different lift-off criteria are considered: i) the height at which the mass fraction of OH becomes 0.0004 [32], ii) the height at which the mass fraction of OH becomes 0.0006 [33], iii) the location at which the mean temperature reaches 1000 K [34] and iv) the height at which methane reaction rate goes over 1% [35]. Table 1 shows the lift-off predictions using these different criteria for the three Reynolds numbers. Also included in Table 1, are the results obtained in the previous DCSE study for the same flames [9]. Whatever criterion selected, the trends in the lift-off height predictions

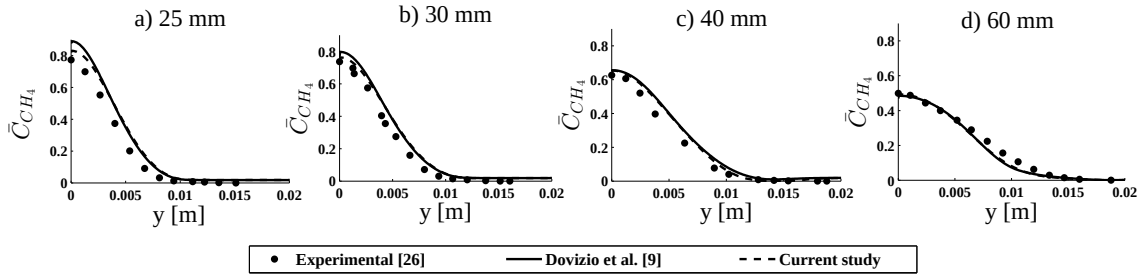

Figure 1: Predictions of radial profiles of methane concentration using the advanced scalar dissipation rate model (Eq. 8) and the algebraic model (Eq. 7) [9] at different axial distances downstream from the jet inlet.

remain the same and the relative difference between the lowest and largest predicted lift-off height range from 15% for Re = 7000 to 21% for Re = 12,000, consistent with what is reported in previous work [9]. It is also clear that the scalar dissipation rate model has an impact on the lift-off height predictions, in particular for the two largest Reynolds numbers. Keeping the first criterion based on the OH mass fraction [32], the differences between the current lift-off height predictions and those reported by Dovizio et al. [9] are 7%, 15% and 29% for Re = 7000, Re = 12000 and Re = 19500, respectively.

Table 1: Lift-off heights in mm for different criteria obtained in the current study using Eq. 8 and previous work using Eq. 7 [9].

Criterion	Re =7000		Re = 12000		Re = 19500	
	Dovizio et al.[9]	Current study	Dovizio et al.[9]	Current study	Dovizio et al.[9]	Current study
$\tilde{Y}_{OH}$=0.0004	28.5	30.5	73	62	129	92
$\tilde{Y}_{OH}$=0.0006	29.5	31	74.5	64	129.5	92
T= 1000 K	34.5	38	83	75	137.5	100
1% of $\dot{\omega}_{CH_4}$	33.5	35	81.5	68	134	93

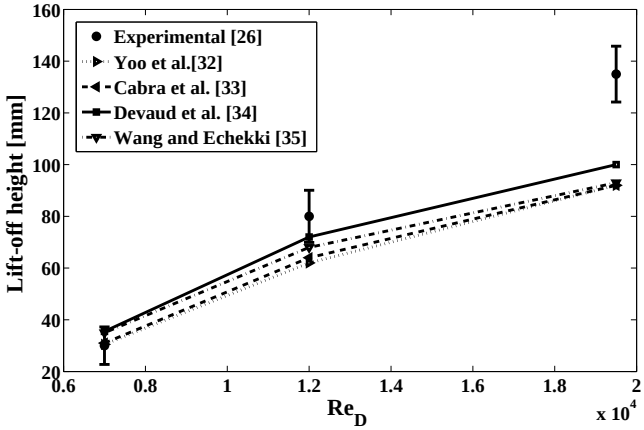

Figure 2: Predicted lift-off heights with different criteria compared with experimental data at three different Reynolds numbers. The bars indicate the rms of fluctuations of the mean lift-off height [26]

For comparison with experimental data, Fig. 2 shows the predicted lift-off values using the different criteria with the experimental values. The experimental lift-off heights are equal to 33 ± 7, 84 ± 11, and 135 ± 11 mm for Re = 7000, 12000, and 19500, respectively. Good agreement is obtained for Re = 7000 as in the previous work using the simple algebraic model, but the current predictions are further away from the experimental values for the two largest Reynolds numbers compared to what is previously obtained. At this stage, it may be concluded that the scalar dissipation rate used in the progress variable variance equation has an impact on the lift-off predictions, in particular for high Reynolds numbers.
The second aspect of the current work is related to the numerical method to solve Eq. 5. Before implementing LSQR in the

DCSE code, a stand-alone code of the LSQR algorithm is used to compare the CPU time to solve Eq. 5 for a given instant and ensemble, with the time needed for the same purpose using LU-decomposition. The same inputs are used for both techniques and the results are presented in Table 2. As shown in Table 2, a significant decrease in the time consumed in the inversion process can be seen when the LSQR algorithm is implemented compared with the originally used LU-decomposition. The LSQR routine adjustable parameters like maximum number of iterations and relative error between results between each two successive iterations are set to 100 and 10^{-10}, respectively. It should be noted that the maximum number of iteration has never been reached for all tested time steps of the three ensembles. The value of $\|A\vec{\alpha} - \vec{b}\|_2$ is used as a measure of the deviation from the exact solution. Thus, as the value of the L2-norm decreases, the solution gets closer to the exact solution. It is interesting to see that the LSQR results show smaller L2-norm values compared to the values obtained using the LU-decomposition which means excellent accuracy is maintained. After inversion, some unphysical negative values are sometimes found, but less often when LSQR is used than when LU-decomposition is selected. The non-physical values are replaced with zeros without affecting the results as they appear for fuel rich mixture fractions where reaction rates are negligible.

Table 2: Comparison between results obtained in solving Eq. 4 using LSQR and LU-decomposition

Ensemble	LU-decomposition		LSQR factorization	
	L2-norm	CPU time (s)	L2-norm	CPU time (s)
1	0.1887	2.66	0.1703	1.17
2	0.3033	1.99	0.2231	1.27
3	0.1287	1.28	0.0487	0.66

Next, the LSQR algorithm is coupled to DCSE. Two identical cases are run from the same starting time and the same initial time step. As shown in Fig. 3, the average time consumed per time-step for LU-decomposition is approximately 10 s, while it is approximately 4 s using LSQR leading to the computational time being reduced by a factor of 2.5 when LSQR is implemented.

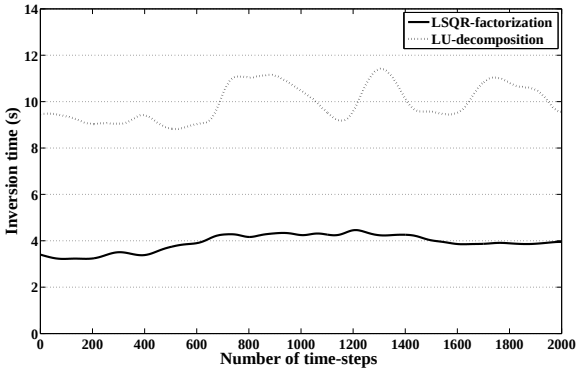

Figure 3: Time spent in the inversion process estimated at each time-step separately for cases using LSQR and LU-decomposition

5. CONCLUSIONS

RANS simulations of a series of lifted turbulent jet flames initially performed by Dovizio et al.[9] were revisited. In the present work, a more advanced scalar dissipation rate formulation [11] was implemented and a different numerical technique was investigated to solve the inverted integral equation. In particular, the Least Squares QR-factorization (LSQR) algorithm instead of LU-decomposition, was examined.

The predictions obtained for the radial profiles of methane concentration at different radial locations have shown good agreement with the experimental results. Different approaches were used to estimate the lift-off height from the numerical results. For the different criteria, the trends in the lift-off height predictions remained the same and the relative difference between the lowest and largest predicted lift-off height ranged from 15% for Re = 7000 to 21% for Re = 12,000, consistent with previous work [9]. The scalar dissipation rate model was shown to have an impact on the lift-off height predictions, in particular for the two largest Reynolds numbers. Keeping the first criterion based on the OH mass fraction [32], the differences between the current lift-off height predictions and those reported by Dovizio et al. [9] with the simple algebraic model were 7%, 15% and 29% for Re = 7000, Re = 12000 and Re = 19500, respectively.

The LSQR algorithm was shown to reduce the inversion computational time by a factor of 2.5, while keeping the the same, if not higher accuracy than the LU decomposition.

Future work will examine the effect of the scalar dissipation rate model for different flames and include the implementation of the DCSE in LES using LSQR.

ACKNOWLEDGMENT

Financial support for this research is provided by the Natural Sciences Engineering Research Council (NSERC) of Canada. The authors would like to thank Prof. Bushe and Mr. Hong Tsui for their help related to the LSQR implementation.

References

[1] K.M. Lyons, Prog. Energ. Combust., 33 (2) (2007) 211-231.
[2] A. Watson, K.M. Lyons, C.D. Carter, J.M. Donbar, Combust. Sci. Technol. 175 (2003) 649 - 664.
[3] S.H. Starner, R.W. Bilger, K.M. Lyons, J.H. Frank, M.B. Long, Combust. Flame 99 (2) (1994) 347 - 354.
[4] K. Su, O.S. Sun, M.G. Mungal, Combust. Flame 144 (2006) 494 - 512.
[5] L. Muniz, M.G. Mungal, Combust. Flame 111 (1997) 16 - 31.
[6] D. Bradley, P.H. Gaskell, A.K. C Lau, Proc. Combust. Inst. 23 (1990) 685 - 692.
[7] D. Bradley, P.H. Gaskell, X.J. Gu, Proc. Combust. Inst. 27 (1998) 1199 - 1206.
[8] M. Chen, M. Herrmann, N. Peters, Proc. Combust. Inst. 28 (2000) 67 - 174.
[9] D. Dovizio, J.W. Labahn, C.B. Devaud, Combust. and Flame 162 (5) (2015) 1976 - 1986.
[10] D. Dovizio, A. Debbagh, and C.B. Devaud. Flow Turbul. Combust., in press, 2015.
[11] Daniele Dovizio, Doctoral dissertation, University of Waterloo, (2015).
[12] E. Lee, H. Huang, J.M. Dennis, P. Chen, L. Wang., Comp. and Geos. 61 (2013) 184 - 197.
[13] A.Yu. Klimenko, R.W. Bilger, Prog. Energy Combust. Sci. 25 (6) (1999) 595 - 687.
[14] M. Wang, J. Huang, W.K. Bushe, Proc. Combust. Inst. 31 (2007) 1701 - 1709.
[15] R. Grout, W.K. Bushe, C. Blair, Combust. Theory, Model. 11 (2007) 1009 - 1028.
[16] J.W. Labahn, C.B. Devaud, Combust. Theory Model. 17 (5) (2013) 960 - 982.
[17] M.M. Salehi, K.J. Daun, W.K. Bushe, Combust. Theory Model. 16 (2012) 301 - 320.
[18] D. Dovizio, M.M. Salehi, C.B. Devaud, Combust. Theory Model. 17 (5) (2013) 935 - 959.
[19] P.C. Hansen, Inverse Problems 8 (1992) 849 - 872.
[20] S.S. Girimaji, Combust. Sci. Technol. 78 (1991) 177 - 196.
[21] B. Jin, R. Grout, and W.K. Bushe. Flow Turbul. Combust., 81:563–582, 2008.
[22] A.N. Tikhonov, V.Y. Arsenin, Halsted Press, Washington (1977).
[23] C. C. Paige and M. A. Saunders, ACM Trans. Math. Softw. 8 (1982) 43-71.
[24] G. Golub and W Kahan, Journal of the Society for Indus. and App. Math. B 2 (1965) 205-224.
[25] R.W. Schefer, P.J. Goix, Combust. Flame 112 (1998) 559 - 574.
[26] R.W. Schefer, M. Namazian, J. Kelly, Combust. Flame 99 (1994) 75 - 86.
[27] M. Namazian, R.W. Schefer, J. Kelly, Combust. Flame 74 (2) (1988) 147 - 160.
[28] OpenFOAM (The open source CFD toolbox).
[29] B.E. Launder, B.I. Sharma, Lett. Heat Mass Transfer 1 (1974) 131 - 138.
[30] S.B. Pope, U. Maas, Cornell University Report No FDA (1993) 93-11 .
[31] H. Kolla, J. Rogerson, N. Chakraborty and N. Swaminathan, Combust. Sci. Tech. 181 (3) (2009) 518-535.
[32] C.S. Yoo, E.S. Richardson, R. Sankaran, J.H. Chen, Proc. Combust. Inst. 33 (1) (2011) 1619 - 1627.
[33] R. Cabra, T. Myhrvold, J.Y. Chen, R.W. Dibble, A.N. Karpetis, R.S. Barlow, Proc. Combust. Inst. 29 (2002) 1881 - 1888.
[34] C.B. Devaud, J.H. Kent, R.W. Bilger, Proc. of the 3rd Mediter. Combust. Symp. (2003) 972 - 981.
[35] W. Wang, T. Echekki, Fire Safety J. 46 (2011) 254 - 261.